SEMARAK ILMU PUBLISHING

Journal of Advanced Research in Numerical Heat Transfer

Journal homepage:
https://semarakilmu.com.my/journals/index.php/arnht/index
ISSN: 2735-0142

Modeling of Electric MHD Flow of Nanoparticles in a CMC-Water Based Casson Hybrid Nanofluid over a Porous Medium

Hamzeh Taha Alkasasbeh[1,2,*], Feras A. Hanandeh[3,4], Bajes Z. Aljunaeidia[3], Nesreen M. Al-Olaimat[2], Abduallah M. Alzyout[2], Sara A. Khalil[1], Muhammad Khairul Anuar Mohamed[5]

[1] Mathematics Department, Faculty of Science, Applied Science Private University (ASU) Amman, Jordan
[2] Department of Mathematics, Faculty of Science, Ajloun National University, P.O. Box 43, Ajloun 26810, Jordan
[3] Department of Computer Science, Faculty of Information Technology, Ajloun National University, P.O. Box 43, Ajloun 26810, Jordan
[4] Department of Computer Information Systems Faculty of Prince Al-Hussein Bin Abdallah II for Information Technology, Hashemite University, P.O. Box 150459, Zarqa 13115, Jordan
[5] Centre for Mathematical Sciences, Universiti Malaysia Pahang, Persiaran Lebuhraya Tun Khalil Yaakob, Kuantan, Pahang, 26300, Malaysia

ARTICLE INFO

Article history:
Received 15 June 2024
Received in revised form 19 July 2024
Accepted 18 August 2024
Available online 30 September 2024

Keywords:
Casson Fluid; Hybrid Nanofluid; Electric MHD; Stretching Sheet; Porous Medium

ABSTRACT

The principal focus of this exploration is to study the computationally simulate the combined convection of CMC-water-based Casson hybrid nanofluid through a stretching sheet with electric magnetic force in a porous medium. Copper (Cu) and Silver (Ag) nanoparticles are included to enhance the heat transfer performance of CMC-water. The physical problem is formulated with mathematical PDEs, and to solve this, initially we used similarity transformation technique to reduce the PDEs into ODEs, then Runge-Kutta Fehlberg method (RKFM) of order four with shooting technique is adopted for further reduction from the non-linear ODEs to first order DEs. The influence of key parameters such as the magnetic field parameter (M), porous medium parameters (K), electric field factor (E), radiation parameter (Nr), permeability parameter (λ), Casson parameter (β), and Eckert number (Ec) on relevant physical quantities is illustrated through tables and graphical visualizations. The impact of these parameters on velocity and temperature profiles, as well as on the skin friction coefficient and Nusselt number of the nanofluid, is observed. Our results indicate that an increase in the Casson parameter values leads to a decrease in the velocity of the host fluid in the case of opposite flow, and a similar behavior is observed with the nanoparticle porous medium parameter (K) in the case of assisting flow. Furthermore, the use of the Runge-Kutta Fehlberg Method (RKFM) is found to be more accurate and reliable in dealing with the problem studied in this work.

1. Introduction

Non-Newtonian fluids, characterized by varying viscosity with shear rate, often have high densities and viscosities, making them challenging to flow through. To overcome this, these fluids can be induced to flow through changes in temperature, pressure, or radiation. The Casson model, a non-Newtonian fluid model with yield stress and shear-thinning properties, is particularly useful. This

* *Corresponding author.*
E-mail address: alkasasbehh@gmail.com (Hamzeh Taha Alkasasbeh)

https://doi.org/10.37934/arnht.24.1.2844

model is favored for human blood due to its unique characteristics, such as causing red blood cells to form rouleaux under yield stress conditions. The Casson model is instrumental in understanding the flow behavior of complex fluids like blood, where yield stress plays a crucial role in determining flow properties [1].

The Casson fluid model, a subcategory of non-Newtonian fluid, is extensively used to study the behavior of complex fluids like blood. This model is particularly relevant for understanding blood flow characteristics, especially at minimal shear rates, where blood moves through small blood arteries [2]. The Casson model is favored for simulating blood flow due to its ability to describe the behavior of blood under various conditions, including temperature, hematocrit levels, and the presence of anticoagulants [3]. Studies have shown that blood exhibits characteristics similar to Casson fluids, behaving like a solid under yield stress conditions and transitioning to a liquid state to flow [4]. Researchers have compared the Casson model with other fluid models like the Herschel-Bulkley model, highlighting the Casson model's accuracy in describing blood rheology, especially in scenarios involving moderate shear rates. The Casson fluid model is crucial for understanding the flow dynamics of blood in different situations, making it a valuable tool in medical and chemical industries for studying fluid behavior in various applications [5].

Following these findings, several research studies have delved deeper into the same field. Mustafa *et al.,* [6] conducted research focusing on another aspect of the subject. Additionally, Mustafa *et al.,* [7] explored the parallel free stream's dynamics in the presence of Casson fluid on a semi-infinite flat plate. Furthermore, Nadeem *et al.,* [8] investigated the boundary layer flow characteristics of Casson fluid in a three-dimensional context on a stretching sheet. These studies contribute to a broader understanding of Casson fluid behavior and its applications in various flow scenarios, other research on Casson fluids can also be found in the literature from the previous study [9-16].

The industrial applications and significant impact on various technological processes of laminar flow and heat transfer over a stretching sheet in a viscous fluid are subjects of great interest in academia. Studies have shown that factors like viscosity, thermal conductivity, magnetic parameters, and temperature ratios play crucial roles in influencing heat transfer rates, skin friction, and Nusselt numbers in these scenarios [17-20].

In much of the existing literature, the focus has been on studying a stretching surface under the assumption that the surface's velocity is linearly proportional to the distance from a fixed origin. However, Gupta and Gupta [21] have pointed out that this assumption of linear stretching may not always hold true, especially in the case of plastic sheet stretching.

A few years later, several studies examined heat mass transfer on boundary layer flows, including Magyari and Keller [22], Elbashbeshy [23], Partha *et al.,* [24], Khan [25], Sanjayanand and Khan [26]. These studies mentioned in the sources focus on boundary layer flow and heat transfer over various types of surfaces. Specifically, the research delves into phenomena like boundary layer flow due to exponential shrinking or stretching of sheets, nanofluid past a stretching/shrinking sheet, and slip flow past a porous flat plate. These studies employ numerical methods to analyze the effects of parameters like suction, permeability, slip, and magnetic fields on velocity, temperature, and mass transfer rates. The findings highlight how these parameters influence heat transfer, fluid flow, and concentration fields in different scenarios, providing insights into technological applications such as annealing and thinning copper wires. Additionally, the impact of thermophysical conditions on flow and heat transfer through exponentially stretching sheets is explored, emphasizing the significance of these processes in determining the quality of finished products. Subsequently, Sajid and Hayat [27] employed the Homotopy analysis method (HAM) to analytically solve the problem and investigate the influence of thermal radiation on the boundary layer flow generated by an exponentially stretching sheet. Similarly, Bidin and Nazar [28] recently conducted an analysis on the impact of thermal radiation on heat transfer across an exponentially stretched sheet, focusing on constant laminar two-dimensional boundary layer flow. Additionally, Bararnia *et al.,* [29] conducted an analytical investigation into the boundary layer flow and heat transfer on a continuously stretched surface. These studies contribute to a deeper understanding of the effects of thermal radiation and stretching surfaces on fluid flow and heat transfer phenomena.

A nanofluid is a base fluid with nanoparticles suspended in it, enhancing its heat transfer properties significantly. These nanoparticles can be of various types, such as polymeric, metallic, or non-metallic particles [30]. In contrast, slurries typically contain larger particles, ranging from millimetres to micrometres, which can lead to significant challenges. The use of nanofluids offers improved thermal conductivity and heat transfer coefficients compared to base fluids, making them valuable for applications in heat exchangers and various heat transfer devices. The studies reviewed emphasize the benefits of nanofluids in enhancing heat transfer efficiency and highlight their potential in improving the performance of heat exchangers and other thermal systems [31]. In real-world applications, the motion of nanoparticles in fluids can lead to an increase in pressure drop. Xuan and Li [32] as well as Choi and Eastman [33] introduced the term "nanofluid" to describe artificial colloids composed of nanoparticles dispersed within a base fluid. Lee *et al.,* [34] conducted experiments to determine the thermal conductivities of oxide nanofluids. The experimental results demonstrated a significant enhancement in the thermal conductivity of the base fluid when nanoparticles were suspended in it. This improvement is attributed to the behavior of the nanofluid, which tends to exhibit more fluid-like properties rather than behaving like a typical solid-fluid combination. Li *et al., [35]* examined heat transfer near a Stagnation Point of a Maxwell nanofluid flow passing over a porous rotating disk.

Hybrid nanofluids are advanced colloidal suspensions that combine multiple nanoparticles with a base fluid, aiming to enhance thermal properties beyond those of conventional nanofluids [36]. These innovative fluids address the limitations of mono nanofluids by incorporating diverse nanoparticles like metals, crystalline oxides, ceramic oxides, and carbon-based particles. The synthesis of hybrid nanofluids involves various methods depending on the nanoparticles used, offering a tailored approach for specific applications in heat transfer [37]. Devi and Devi [38] studied on the flow of hybrid nano elements composition along a stretching surface. Stagnation point flow over a stretching/ shrinking cylinder by hybrid nanofluid was investigated by Waini *et al.,* [39]. Waqas *et al.,* [40] studied on hydro magnetic flow of hybrid nanofluids past a vertical stretching cylinder. Effects of thermal radiation and viscous dissipation on hybrid nanofluid through a circular cylinder was explored by Roy *et al.,* [41]. Other interesting studies on nanofluids and hybrid nanofluids can be found in Refes [42-46].

The prominent intension and originality of this present study is on hybrid nanofluid composition fluid along a stretching sheet with Casson fluid model by considering CMC-water as base fluid with Cu and Ag as its hybrid nano-composition to understand the effect of variable dissipation, radiation and electric MHD on fluid momentum and energy under the influence of Boussinesq approximation with constant/prescribe wall temperature. The electric MHD flow of this Casson hybrid nanofluid in porous medium is a new work as per the reviewed literature and this paper can have a greater scope in the future industrial applications.

The following points highlight the novelty of this article:

i) The use of Silver (Ag) and copper (Cu) nanoparticles with CMC-water as base fluid is considered.
ii) Thermal radiation is treated nonlinearly, and electric MHD is taken into consideration.

iii) Thermal characteristics of nanofluid Cu /CMC-water and hybrid Ag+Cu/CMC-water Casson nanofluid are compared and finding.

2. Mathematical Modeling

In this study, we examine the 2D flow of a Casson hybrid nanofluid with incompressible and free convection characteristics, affected by CMC-water and thermal radiation, on a stretching sheet. The boundary condition includes a constant wall temperature. Our analysis includes the effects of thermal radiation, thermophoresis and electric magnetic force in porous medium on the transport of mass and heat transfer. We utilize two perpendicular coordinate systems (*x, y*) due to the sheet's motion along the *x*-axis and the noncompressible nature of the wall ($v_w = -\frac{1}{2}\sqrt{\left(\frac{U_\infty v_f}{x}\right)}\lambda$), as illustrated in Figure 1 .

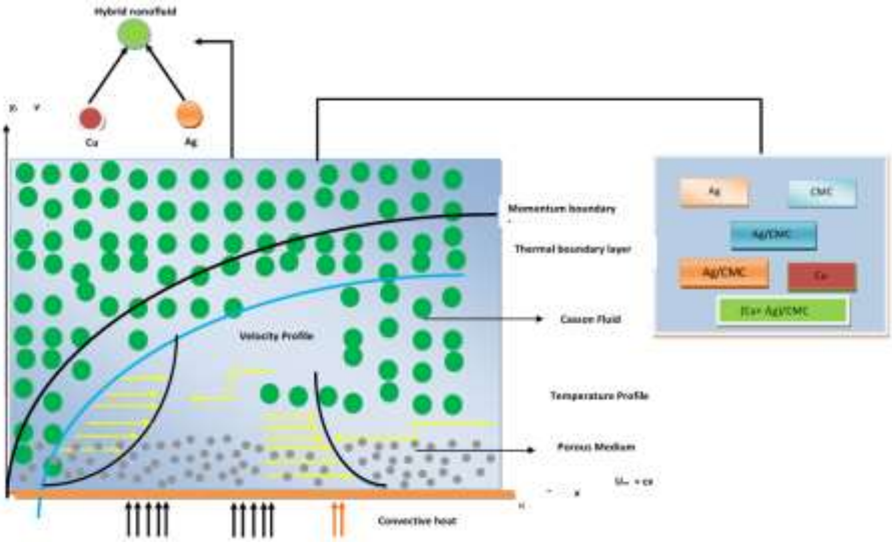

Fig. 1. Geometry of the problem

A Casson fluid, as described by Casson in 1959, is a non-Newtonian fluid known for its shear-thinning behavior and infinite viscosity at zero shear rate. This fluid type has distinctive flow characteristics that find applications in biomedical and industrial contexts. The basic equations governing an incompressible Casson fluid with isotropic properties are expressed as follows [14]:

$$\tau_{ij} = \begin{cases} 2(\mu_B + P_y/\sqrt{2\pi})e_{ij} & \pi > \pi_{c,} \\ 2(\mu_B + P_y/\sqrt{2\pi_c})e_{ij} & \pi < \pi_{c,} \end{cases}, \tag{1}$$

Here, the symbols represent the following quantities: μ_B is the plastic dynamic viscosity, P_y is the yield stress, e_{ij} is the deformation direction component rate, π is the product of the component of the rate of deformation with itself ($e_{ij}e_{ij}$), and π_c is the critical value of the product of the component of the strain tensor rate with itself.

Based on the assumptions mentioned earlier, the governing equations along with their corresponding boundary conditions can be expressed as follows [47,48]:

$$\frac{\partial u}{\partial x} + \frac{\partial v}{\partial y} = 0 \tag{2}$$

$$u\frac{\partial u}{\partial x}+v\,\frac{\partial u}{\partial y}=V_{hnf}(1+\tfrac{1}{B})\frac{\partial^2 u}{\partial y^2}+\frac{\sigma_{hnf}}{\rho_{hnf}}(\beta_0 E_0-\beta_0^2 u)-\frac{V_{hnf}}{K^*}u\,, \tag{3}$$

$$u\frac{\partial T}{\partial x}+v\frac{\partial T}{\partial y}=\frac{k_{hnf}}{(\rho C_p)_{hnf}}\frac{\partial^2 T}{\partial y^2}-\frac{1}{(\rho C_p)_{hnf}}\frac{\partial q_r}{\partial y}+\frac{\mu_{hnf}}{(\rho C_p)_{hnf}}\frac{u}{K^*} \tag{4}$$

with BCs

$$u\rightarrow U_\infty=cx\,,v=v_w\,,T=T_w(x)\,,at\;\;y=0,$$
$$u=0\,,T\rightarrow T_\infty\;as\;y\rightarrow\infty\;\;. \tag{5}$$

By applying the Roseland approximation, the radiative heat flux at this particular point can be determined.

$$q_r=-\frac{4\sigma^*}{3k^*}\frac{\partial T^4}{\partial y}; \tag{6}$$

Here, σ^*, qr, and k^* represent the Boltzmann constant, absorption coefficient, and radiative heat flux, respectively. Assuming a small temperature variation in the flow, the Taylor series approximation for T^4 in terms of T_∞ can be obtained as follows:

$$T^4\cong 4TT_\infty^3-3T_\infty^3 \tag{7}$$

$$\frac{\partial q_r}{\partial y}=\frac{16\sigma^* T_\infty^3}{3k^* v_f(\rho C_p)_f}\frac{\partial^2 T}{\partial y^2} \tag{8}$$

Table 1 demonstrates the thermophysical relation of hybrid nanofluids [14, 47] where ϕ_1 and ϕ_2 are the nanoparticle volume fraction for Cu and Ag, respectively.

Table 1
Thermo-physical properties of hybrid nanofluid and nanoparticles [14, 47]

Properties	Hybrid nanofluid
Dynamic Viscosity (μ)	$\frac{\mu_{hnf}}{\mu_f}=\frac{1}{(1-\phi_1)^{2.5}(1-\phi_2)^{2.5}}$
Density (ρ)	$\frac{\rho_{hnf}}{\rho_f}=\left[(1-\phi_2)\left\{(1-\phi_1)\rho_f+\phi_1\frac{\rho_{s1}}{\rho_f}\right\}\right]+\phi_2\frac{\rho_{s2}}{\rho_f}$
Heat Capacity *(ρC_ρ)*	$\frac{(\rho c_p)_{hnf}}{(\rho c_p)_f}=\left[(1-\phi)_2\left((1-\phi_1)+\frac{\phi_1(\rho C_p)_{s1}}{(\rho C_p)_f}\right)+\phi_2\frac{(\rho C_P)_{s2}}{(\rho C_p)_f}\right]$
Thermal Conductivity (k)	$\frac{K_{hnf}}{K_f}=\frac{(K_{s2}+2K_{bf})-2\phi_2(K_{bf}-K_{s2})}{(K_{s2}+2K_{bf})+\phi_2(K_{bf}-K_{s2})}$ where $\frac{K_{bf}}{K_f}=\left[\frac{(K_{s1}+2K_f)-2\phi_1(K_f-K_{s1})}{(K_{s1}+2K_f)+\phi_1(K_f-K_{s1})}\right]$
Electrical Conductivity (σ)	$\frac{\sigma_{hnf}}{\sigma_f}=\left[1+\frac{3\phi_1\left(\sigma_1\phi_1+\sigma_2\phi_2-\sigma_{bf}(\phi_1+\phi_2)\right)}{(\sigma_1\phi_1+\sigma_2\sigma_2+2\phi\sigma_{bf})-\phi\sigma_{bf}\left((\sigma_1\phi_1+\sigma_2\phi_2)-\sigma_{bf}(\phi_1+\phi_2)\right)}\right]$

The following similarity transformations are used to convert PDEs to ODEs.

$$\eta=y\left(\frac{u_\infty}{v_f x}\right)^{1/2},\psi\;=\;\left(u_\infty v_f x\right)^{1/2}f(\eta)\,,\theta(\eta)\;=\;\frac{T-T_\infty}{T_w-T_\infty} \tag{9}$$

where ψ is the stream function defined as $v = \frac{\partial \psi}{\partial x}$ and $u = \frac{\partial \psi}{\partial y}$.

When applying the previously mentioned relations, Eq. (2) is immediately fulfilled. Furthermore, Eqs. (2-4) can be condensed into dimensionless form as follows

$$A_1(1+\frac{1}{\beta})f'''(\eta) + A_2 f(\eta)f''(\eta) - A_2\left(f'(\eta)\right)^2 + A_3 M\left(E - f'(\eta)\right) - A_1 K f'(\eta) = 0 \tag{10}$$

$$\frac{1}{\Pr}\frac{1}{A_5}\left(A_4 + \frac{4}{3}Rd\right)\theta''(\eta) + f(\eta)\theta'(\eta) + \frac{A_1}{A_5}\,Ec\,K\,f'(\eta) = 0 \tag{11}$$

where $A_1 = \frac{\mu_{hnf}}{\mu_f}$, $A_2 = \frac{\rho_{hnf}}{\rho_f}$, $A_3 = \frac{\sigma_{hnf}}{\sigma_f}$, $A_4 = \frac{K_{hnf}}{K_f}$, $A_5 = \frac{(\rho C_p)_{hnf}}{(\rho C_p)_f}$, $M = \frac{\sigma_f \beta_0^2}{a\rho_f}$ is magnetic parameter, $E = \frac{E_o}{c\,x\,\beta_o}$ is electric paremeter, $K = \frac{\mu_f}{\rho_f k^* c}$ is the porous medium parameters, $\Pr = \frac{v_f(\rho C_p)_f}{K_f}$ is Prandtl number, $\mathrm{Ec} = \frac{\mathrm{C}^2 x}{(\rho C_p)_f (T_w - T_\infty)}$ is the Eckert number, β is Casson paremeter, β_o is strength of magnetic field and $\mathrm{Rd} = \frac{4\sigma^* T_\infty^3}{K^* K_f}$ is Radiation parameter.

For a similarity solution to exist for Eqs. (2) to (5):

$$v_w = -\frac{1}{2}\sqrt{\left(\frac{U_\infty v_f}{x}\right)}\lambda \tag{12}$$

where λ is permeability rate at the plate surface constant.

The non-dimensional boundary conditions (5) are as follows

$$\begin{aligned} &f = \lambda, f' = 0, \theta = 1 \quad \text{at} \quad \eta = 0, \\ &\quad f' \to 1, \quad \theta \to 0, \ as\ \eta \to \infty. \end{aligned} \tag{13}$$

The dimensionless physical quantities of importance are the skin friction coefficient Cf and the Nusselt number Nu which are expressed mathematically as:

$$Cf = \left(1 + \frac{1}{\beta}\right)\frac{\mu_{hnf}}{U_w^2 \rho_f}\left(\frac{\partial u}{\partial y}\right)_{y=0} \qquad Nu = \frac{x k_{hnf}}{k_{f(T_w - T_\infty)}}\left(\frac{\partial T}{\partial y}\right)_{y=0} + (q_r)_{y=0} \tag{14}$$

The non-dimensional skin friction coefficient and Nusselt number obtained by applying (6) and (9) in (14), are as follows:

$$Re_x^{\frac{1}{2}} Cf = A_1\left(1 + \frac{1}{\beta}\right)f''(0), \; Re_x^{-\frac{1}{2}} Nu = -\left(A_4 + \frac{4}{3}Rd\right)\theta'(0) \tag{15}$$

3. Numerical Approach

The set of non-dimensional ODEs are worked out with the help of Runge-Kutta method with the technique of shooting method, wherein the system of non-linear ODEs is rephrased into the corresponding system of first order ODEs by using the substitutions. The variables in this study are defined as:

$$f(\eta) = X_1 \ , \ \frac{\partial f}{\partial \eta} = X_2 \ , \ \frac{\partial^2 f}{\partial^2} = X_3 \ , \theta(\eta) = Y_1 \ , \ \frac{\partial \theta}{\partial \eta} = Y_2 \tag{16}$$

By using equation (13) in equations (7) -(9) then the system of ODEs are reduced as follows:

$$\begin{pmatrix} X'_1 \\ X'_2 \\ X'_3 \\ Y'_1 \\ Y'_2 \end{pmatrix} = \begin{pmatrix} X_2 \\ X_3 \\ \frac{1}{A_1\left(1+\frac{1}{\beta}\right)}\left[A_2 X_2^2 \ - A_2 X_1 X_3 - A_3 M(E - X_2) - A_1 K X_2\right] \\ Y_2 \\ -\frac{\Pr A_5}{\left(A_4 + \frac{4}{3} Rd\right)}\left[X_1 Y_2 + \frac{A_1}{A_5} \ Ec \ K \ X_2\right] \end{pmatrix} \tag{17}$$

with boundary conditions

$$X_2(0) = 0 \ , \ X_1(0) = \lambda \ , Y_1(0) = 1 \ , \\ X_1(\infty) = 1 \ , \ Y(\infty) \to \ 0 \tag{18}$$

Runge-Kutta 4th order manner is applied for solving the system of these equations. The chosen upper limit for η_∞ is set at 6. The process of iterative solving continues until convergence is achieved, with a tolerance threshold of 10^{-6} being employed. A numerical code, integrating the methods discussed earlier, was developed using Maple software to address these problems effectively.

4. Numerical Results and Discussions

This section specifies to use numerical computations through Maple software in order to demonstrate the behaviour of two types of nanoparticles, specifically copper nanoparticles (Cu) and silver nanoparticles (Ag), suspended in a Casson hybrid nanofluid comprised of CMC-water as the base fluid. For the hybrid nanofluid, the thermophysical properties of the base fluid and hybrid nanoparticles are displayed in Table 2.

Table 2
Thermo-physical properties of CMC-water (0.0–0.4%) and metals nanoparticle[10]

Thermo-physical property	CMC-Water	Ag	Cu
$\rho(kg/m^3)$	997.1	10,500	8933
$C_p(J/kgK)$	4179	235	385
$\mathrm{K}^{\propto}(w/mK)$	0.613	429	401
$\sigma(s/m)$	5.5×10^{-6}	63×10^{6}	95.6×10^{6}
Pr	6.2	-	-

The qualitative results will be presented empirically by way of graphs and numerical results as well. A visual representation of the influence of relevant parameters on velocity and temperature can be found in Figures 2 through 11. Furthermore, the skin friction coefficient values obtained in this study were compared with those from previous studies on nanofluids, as shown in Table 3. Additionally, Table 4 presents the calculated values for the skin friction coefficient and local Nusselt number.

Table 3 presents the numerical results, which show a significant agreement with the data from existing studies. Specifically, we compared our findings with those of Ahmad *et al.,* [48] to demonstrate the validity, accuracy, and precision of our proposed numerical approach for modeling the behaviour of the Casson hybrid nanofluid over a stretched sheet. This comparison further strengthens our confidence in the quality and reliability of the findings presented in this paper.

Table 3
Comparison values of $Re^{1/2}Cf$ for some values of ϕ_1 for Cu- water nanofluid when, $Ec = \lambda = Nr = E = Ec = \phi_2 = 0, \beta \to \infty$

ϕ_1	Ahmad *et al.,* [48] Cu-water	Present Nanofluid
0	0.3321	0.3320990
0.002	0.3355	0.3355124
0.004	0.3390	0.3390214
0.008	0.3459	0.3458912
0.01	0.3494	0.3495141
0.012	0.3528	0.3528001
0.014	0.3563	0.3562511
0.016	0.3597	0.3596810
0.018	0.3632	0.3632011
0.02	0.3667	0.3667110
0.1	0.5076	0.5075912
0.2	0.7066	0.7066145

Table 4
Description of $Re^{-1/2}Nu$ and $Re^{1/2}Cf$ for various value of different parameters

M	K	E	Nr	λ	β	Ec	$Re^{-1/2}Nu$ Hybrid nanofluid	$Re^{1/2}Cf$ Hybrid nanofluid
0.1	0.1	0.5	0.5	0.1	1	0.5	0.512062	0.134780
0.5							0.551044	0.215692
1							0.581449	0.295730
0.1	0.1	0.5	0.5	0.1	1	0.5	0.512062	0.134780
	0.2						0.484597	0.215692
	0.3						0.459282	0.295730
0.1	0.1	0.5	0.5	0.1	1	0.5	0.512062	0.215692
		1					0.537334	0.295730
		2					0.578267	0.420645
0.1	0.1	0.5	0.5	0.1	1	0.5	0.512062	0.215692
			1				0.454588	0.295730
			2				0.385071	0.420645
0.1	0.1	0.5	0.5	0.1	1	0.5	0.512062	0.134780
				0.5			1.177021	0.215692
				1			2.147249	0.295730
0.1	0.1	0.5	0.5	0.1	1	0.5	0.512062	0.295730
					2		0.507280	0.420645
					3		0.505467	0.520156
0.1	0.1	0.5	0.5	0.1	1	0.5	0.512062	0.215692
						1	0.502306	0.295730
						2	0.482795	0.420645

Table 4 compiles the numerical results of the Nusselt number and friction coefficient for various values of the magnetic field parameter (*M*), porous medium parameters (*K*), electric field factor (*E*), radiation parameter (*Nr*), permeability parameter (λ), Casson parameter (β), and Eckert number (*Ec*). This table illustrates the behavior of the hybrid nanofluid under different conditions. Our findings indicate that an increase in the parameters *M, E*, and λ results in a higher percentage of local Nusselt number and skin friction coefficient. Conversely, an increase in *K, Nr, β,* and *Ec* leads to a significant rise in the skin friction coefficient while causing a decrease in the coefficient of local Nusselt number.

Figure 2 illustrates the relationship between the magnetic field parameter (*M*) and temperature profiles in Casson nanofluid flow over a stretching sheet. The observed trend suggests that as the magnetic field parameter (*M*) increases, the temperature decreases. This phenomenon is attributed to the influence of the magnetic field on the flow dynamics, resulting in a reduction in the length of the stretching sheet, a thinner thermal boundary layer, and subsequently lower temperatures along the sheet.

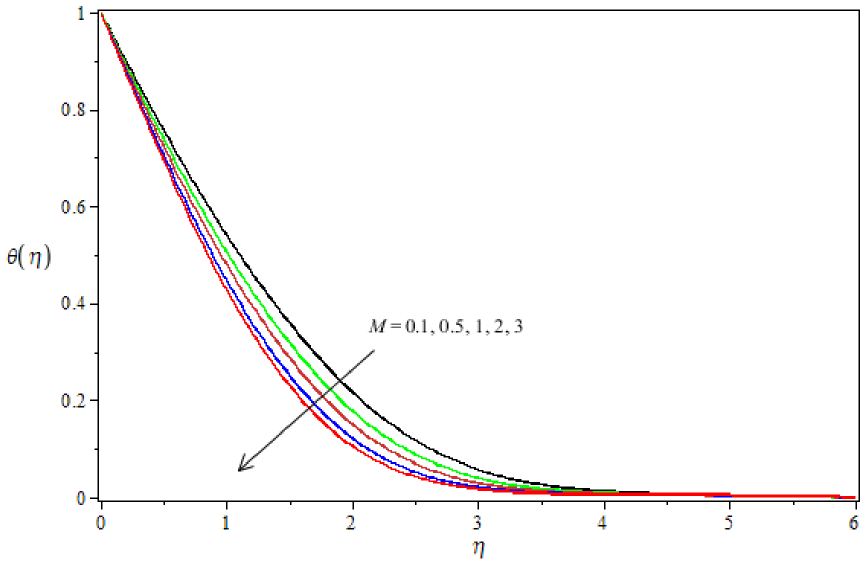

Fig. 2. M versus temperature

Figure 3 shows the temperature profiles for different porous medium parameters (K). With an increase in the parameter of the porous medium, the surface area of the porous medium expands, which allows for a greater space for fluid to flow through the media. The increased surface area leads to a rise in the temperature profile and the thermal boundary layer within the porous medium, affecting the heat transfer characteristics and fluid dynamics.

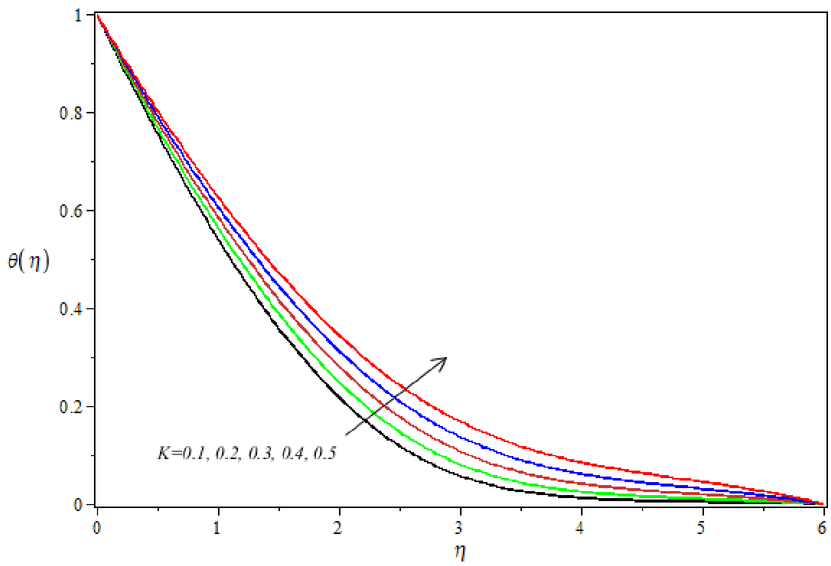

Fig. 3. K versus temperature

At higher values of the electric parameter (E), Figure 4 illustrates a decreasing trend in the temperature profile of the Casson hybrid nanofluid. This decrease in temperature can be attributed to factors such as the increase in momentum layer thickness, thermo-migration effects, and the decrease in thermal conductivity of the Casson hybrid nanofluid. These factors collectively contribute to altering the temperature distribution and thermal behavior of the Casson hybrid nanofluid under the influence of the electric parameter (E).

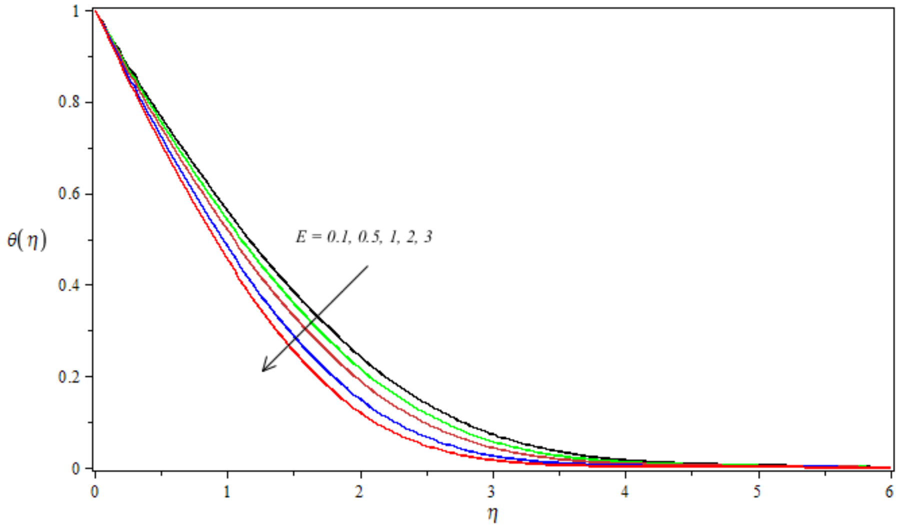

Fig. 4. E versus temperature

In Figure 5, the temperature profiles for different thermal radiation intensities *Nr* are displayed for Casson hybrid nanofluid. The radiation parameter Nr quantifies the relationship between conduction and thermal radiation heat transport mechanisms. A higher value of *Nr* indicates an increased introduction of radiative heat energy into the system, resulting in higher temperatures. Therefore, thermal radiation plays a crucial role in regulating the temperature of boundary layers in the Casson hybrid nanofluid system, impacting heat transfer processes and system dynamics.

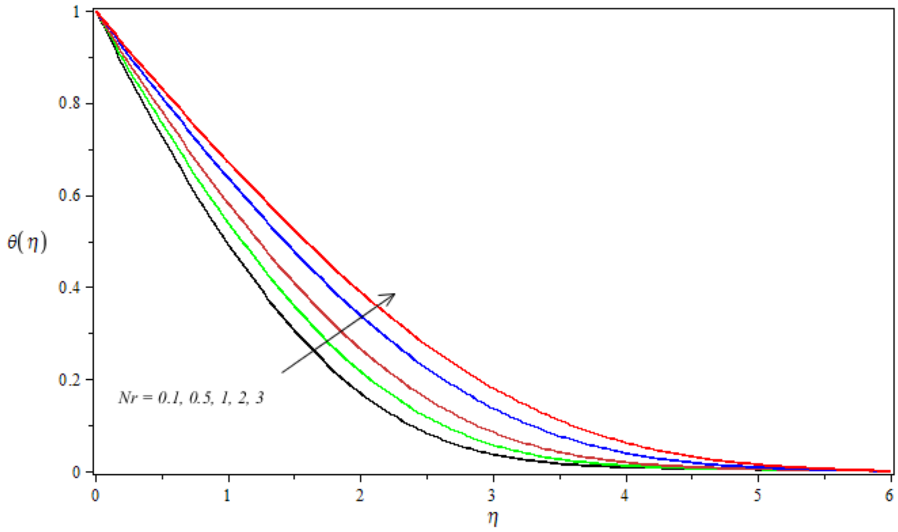

Fig. 5. Nr versus temperature

Figure 6 illustrates the impact of the Eckert number *Ec* on the temperature profile, demonstrating that higher values of the Eckert number lead to an increase in the temperature profile. The Eckert number *Ec* quantifies the relationship between the kinetic energy within the flow and the conversion of this kinetic energy into internal energy through work done against viscous forces. This observation aligns with the understanding that the presence of viscous dissipation effects contributes significantly to increased temperatures within the system.

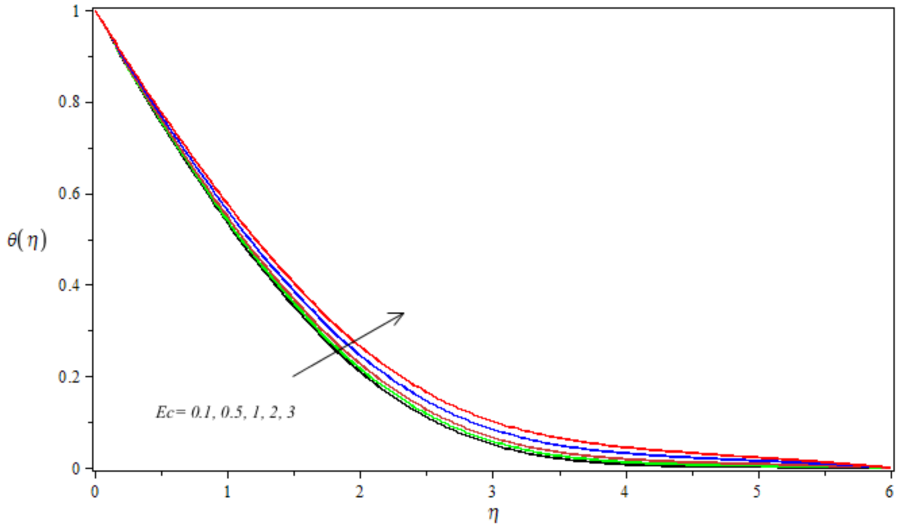

Fig. 6. Ec versus temperature

In Figure 7, the impact of the permeability parameter (λ) on temperature profiles is depicted. The observed trend indicates that as the permeability parameter (λ) increases, the temperature decreases. The relationship mentioned suggests that as the permeability parameter increases, it leads to a reduction in the length of the stretching sheet. This reduction results in a thinner thermal boundary layer along the sheet, which in turn leads to lower temperatures along the sheet's surface. Essentially, higher permeability allows for a more efficient transfer of heat away from the sheet, contributing to cooler temperatures along its length. This phenomenon highlights the significant influence of permeability on the thermal behavior and boundary layer characteristics of the Casson hybrid nanofluid system.

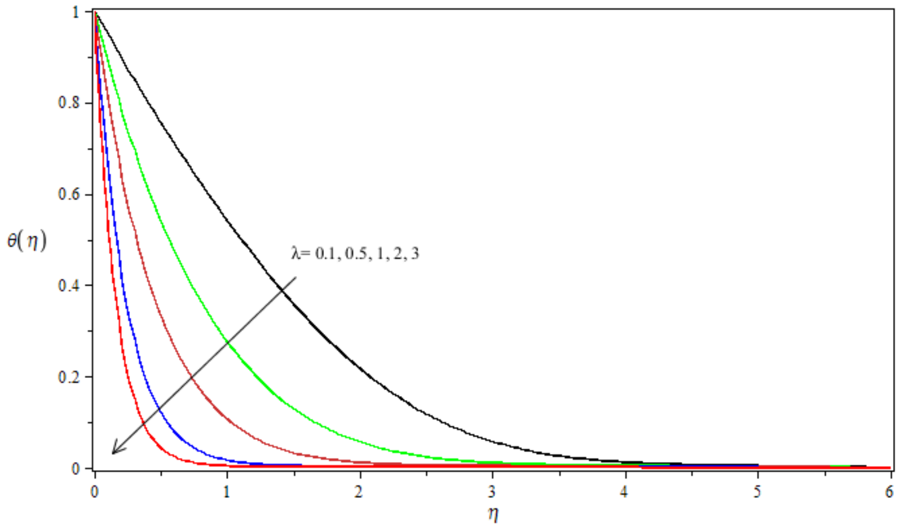

Fig. 7. λ versus temperature

From Figure 8, it is observed that an increase in the Casson parameter (β) leads to a rise in temperature. The trend indicates that higher values of the Casson parameter generate more heat within the system, resulting in an enhanced temperature profile. This relationship underscores the significant impact of the Casson parameter on heat generation and temperature characteristics in Casson nanofluid systems, highlighting the role of this parameter in influencing thermal behavior and heat transfer rates.

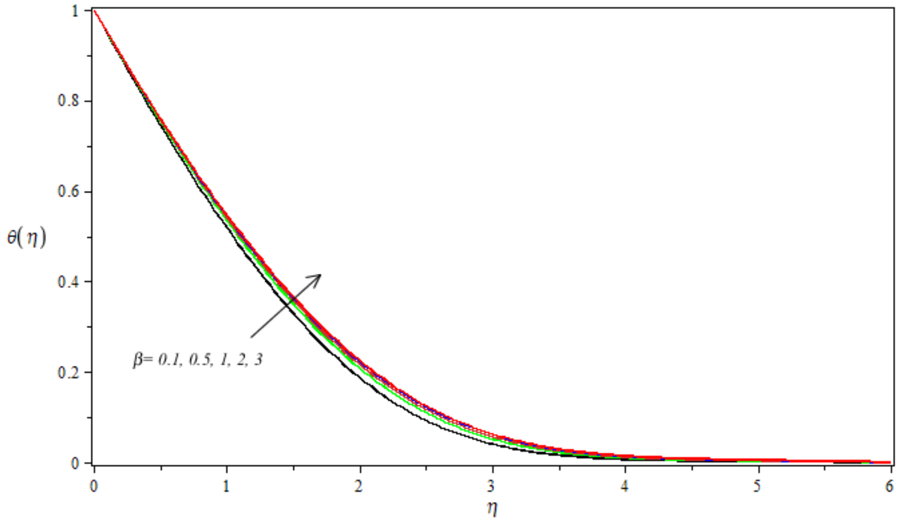

Fig. 8. β versus temperature

In Figure 9, the velocity profiles are displayed with different levels of porosity in the medium. As the porous medium parameter K increases, it indicates that the flow passes through a greater number of randomly oriented pores. Consequently, this leads to a reduction in the thickness of the momentum boundary layer and a decrease in velocity. The presence of porous media increases the contact surface area between the solid and liquid surfaces, thereby influencing the flow characteristics.

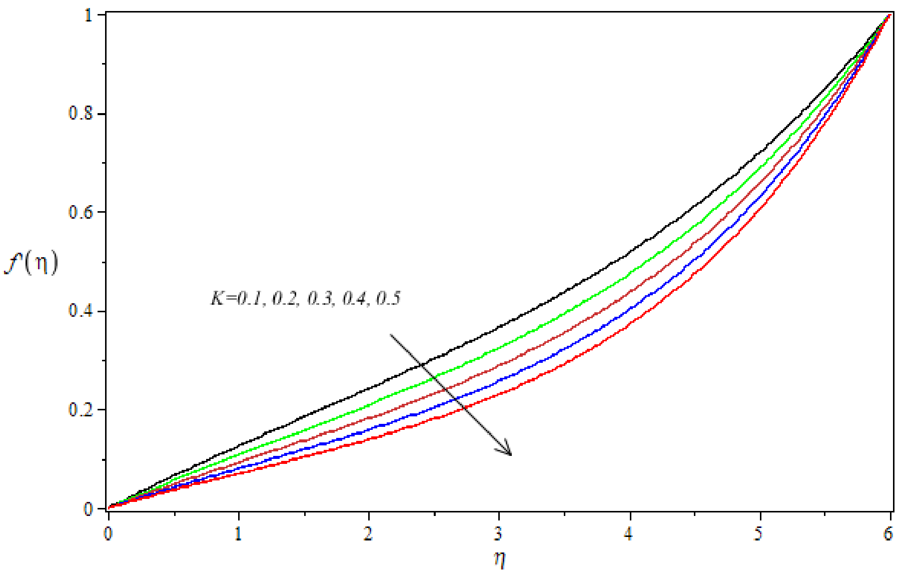

Fig. 9. K versus velocity

In Figure 10, the impact of the electric parameter (E) on velocity is depicted. It is observed that as the value of the electric field parameter increases, the boundary layer velocity also increases. This relationship highlights the significant influence of the electric parameter on velocity profiles in Casson nanofluids, indicating how changes in this parameter impact fluid flow dynamics and boundary layer characteristics.

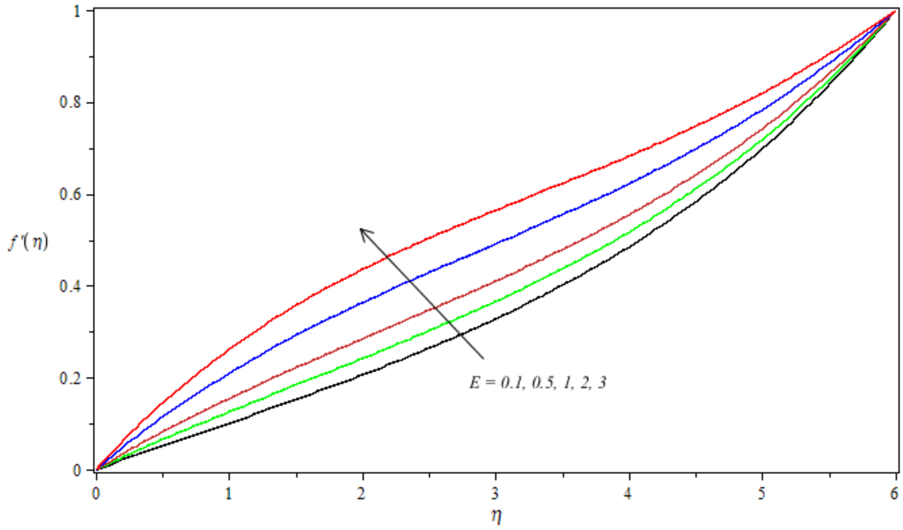

Fig. 10. E versus velocity

From Figure 11, the influence of the permeability parameter (λ) on velocity profiles is depicted. A greater permeability parameter (λ) leads to an increase in velocity due to the reduction in the length of the stretching sheet, resulting in a thinner momentum boundary layer. This reduction in boundary layer thickness diminishes its influence on fluid flow, thereby enhancing the velocity profiles in the Casson hybrid nanofluid system.

Finally, in Figure 12, the effect of the Casson parameter (β) on fluid viscosity is depicted. The increase in the Casson parameter leads to a rise in fluid viscosity, resulting in increased resistance to fluid motion. This observation is supported by the decrease in the velocity profile and boundary layer thickness for higher values of the Casson parameter, highlighting how changes in β impact the fluid dynamics and flow resistance.

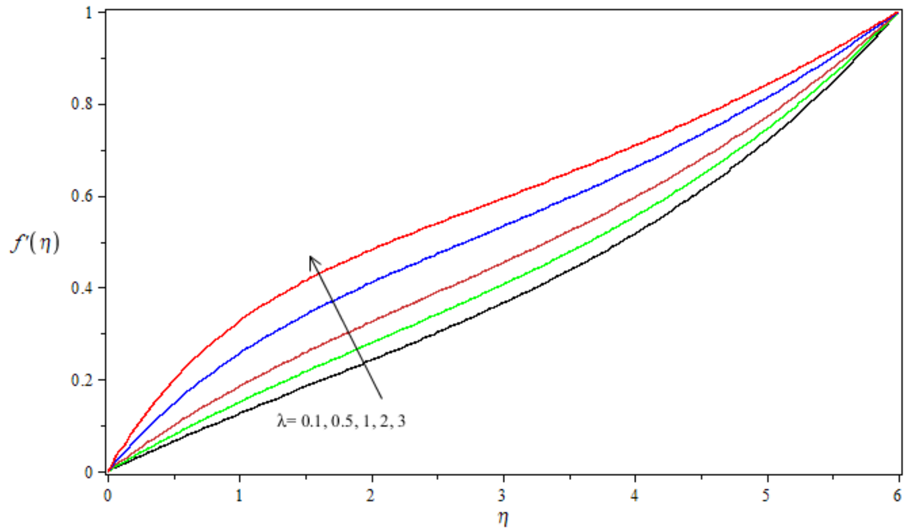

Fig. 11. λ versus velocity

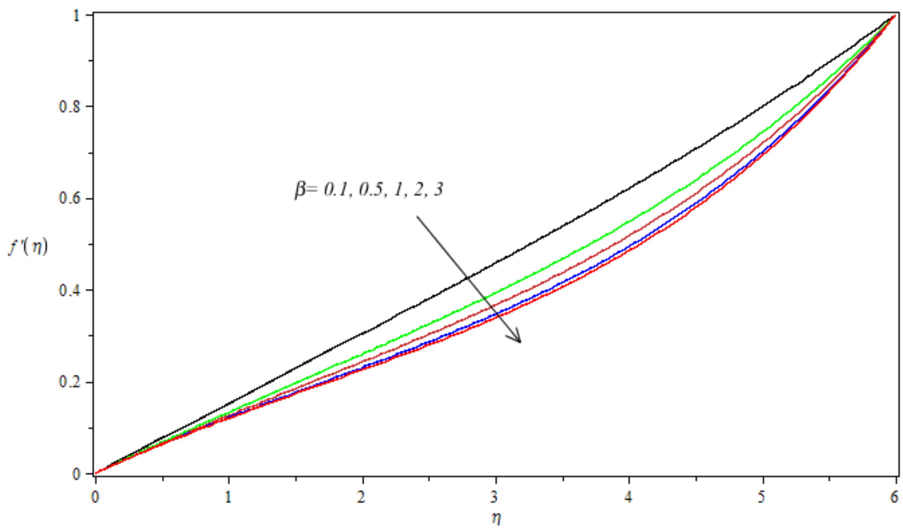

Fig. 12. β versus velocity

5. Conclusion

In this research work, the effect of Casson hybrid nanofluid near a stretching sheet under conditions of constant wall temperature with CMC-water as its base fluid with electric MHD and radiation effects on the flow was considered and solved by using RKFM method in association with "Maple software" to plot the graphs and the tables

Few prominent key points of the study are as follows:

i) Increasing values of the porous medium and Casson parameters lead to a decrease in velocity profiles. These parameters have a negative impact on fluid motion, resulting in lower velocity profiles.
ii) An increase in the electric field factor and permeability parameter has a positive effect on fluid motion, leading to an increase in velocity profiles.
iii) Higher values of the porous medium, radiation, Casson parameters, and Eckert number lead to an increase in temperature. These parameters play a significant role in enhancing heat generation and affecting the temperature distribution in the flow.
iv) The magnetic field parameter, electric field factor, and permeability parameter (λ) are found to decrease temperature profiles with rising values.
v) The Nusselt number increases with higher values of the magnetic field parameter, permeability parameter, and electric field factor. Conversely, it decreases with higher values of the porous medium parameters, radiation parameter, Casson fluid parameter, and Eckert number. These parameters are crucial in influencing convective heat transfer capabilities, which in turn affect the Nusselt number.

Overall, these findings contribute to a better understanding of flow behavior and heat transfer characteristics in Casson hybrid nanofluids, particularly in the context of boundary layer flows near stretching surfaces under various influencing factors. This work can be extended in the future to cover other geometries such as inclined surfaces, disks, cylinders, and spheres.

Acknowledgment
The authors extend their appreciation to the Deanship of Scientific Research at Ajloun National University for funding this work through a large group Research Project.

Reference

[1] Pramanik, S. "Casson fluid flow and heat transfer past an exponentially porous stretching surface in presence of thermal radiation." *Ain shams engineering journal* 5, no. 1 (2014): 205-212. https://doi.org/10.1016/j.asej.2013.05.003 .

[2] Wajihah, S AfiqahSankar DS. "A review on non-Newtonian fluid models for multi-layered blood rheology in constricted arteries." *Archive of Applied Mechanics* 93, no. 5 (2023): 1771-1796. https://doi.org/10.1007/s00419-023-02368-6

[3] Oke, Abayomi S, Mutuku Winifred N, Kimathi Mark, and Animasaun Isaac L. "Insight into the dynamics of non-Newtonian Casson fluid over a rotating non-uniform surface subject to Coriolis force." *Nonlinear Engineering* 9, no. 1 (2020): 398-411. https://doi.org/10.1515/nleng-2020-0025

[4] Jamil, Dzuliana Fatin, Uddin Salah, Kazi Mohsin, Roslan Rozaini, Gorji MR, and Akhir Mohd Kamalrulzaman Md. "MHD blood flow effects of Casson fluid with Caputo-Fabrizio fractional derivatives through an inclined blood vessels with thermal radiation." *Heliyon* 9, no. 11 (2023). https://doi.org/10.1016/j.heliyon.2023.e21780

[5] Shahzad, Hasan, Wang Xinhua, Ghaffari Abuzar, Iqbal Kaleem, Hafeez Muhammad Bilal, Krawczuk Marek, and Wojnicz Wiktoria. "Fluid structure interaction study of non-Newtonian Casson fluid in a bifurcated channel having stenosis with elastic walls." *Scientific Reports* 12, no. 1 (2022): 12219 https://doi.org/10.1038/s41598-022-16213-3

[6] Mustafa, M, Hayat T, Pop I, and Aziz Al. "Unsteady boundary layer flow of a Casson fluid due to an impulsively started moving flat plate." *Heat Transfer—Asian Research* 40, no. 6 (2011): 563-576. https://doi.org/10.1002/htj.20358

[7] Mustafa, Meraj, Hayat Tasawar, Ioan Pop, and Hendi Awatif. "Stagnation-point flow and heat transfer of a Casson fluid towards a stretching sheet." *Zeitschrift für Naturforschung A* 67, no. 1-2 (2012): 70-76. https://doi.org/10.5560/zna.2011-0057

[8] Nadeem, Sohail, Haq Rizwan Ul, Akbar Noreen Sher, and Khan Zafar Hayat. "MHD three-dimensional Casson fluid flow past a porous linearly stretching sheet." *Alexandria Engineering Journal* 52, no. 4 (2013): 577-582. https://doi.org/10.1016/j.aej.2013.08.005

[9] Alwawi, Firas A, Alkasasbeh Hamzeh T, Rashad AM, and Idris Ruwaidiah. "MHD natural convection of Sodium Alginate Casson nanofluid over a solid sphere." *Results in physics* 16 (2020): 102818. https://doi.org/10.1016/j.rinp.2019.102818

[10] Alwawi, Firas A, Alkasasbeh Hamzeh T, Rashad Ahmed M, and Idris Ruwaidiah. "A numerical approach for the heat transfer flow of carboxymethyl cellulose-water based Casson nanofluid from a solid sphere generated by mixed convection under the influence of Lorentz force." *Mathematics* 8, no. 7 (2020): 1094. https://doi.org/10.3390/math8071094

[11] Alkasasbeh, Hamzeh Taha. "Numerical solution of micropolar Casson fluid behaviour on steady MHD natural convective flow about a solid sphere." *Journal of Advanced Research in Fluid Mechanics and Thermal Sciences* 50, no. 1 (2018): 55-66.

[12] Mohamed, Muhammad Khairul Anuar, Yasin Siti Hanani Mat, Salleh Mohd Zuki, and Alkasasbeh Hamzeh Taha. "MHD stagnation point flow and heat transfer over a stretching sheet in a blood-based casson ferrofluid with newtonian heating." *Journal of Advanced Research in Fluid Mechanics and Thermal Sciences* 82, no. 1 (2021): 1-11. https://doi.org/10.37934/arfmts.69.2.118

[13] Mohamed, Muhammad Khairul Anuar, Ishak Anuar, Rosli Wan Muhammad Hilmi Wan, Soid Siti Khuzaimah, and Alkasasbeh Hamzeh Taha. "MHD Natural Convection Flow of Casson Ferrofluid over a Vertical Truncated Cone." *Journal of Advanced Research in Fluid Mechanics and Thermal Sciences* 112, no. 1 (2023): 94-105. https://doi.org/10.37934/arfmts.112.1.94105.

[14] Alkasasbeh, Hamzeh. "Numerical solution of heat transfer flow of casson hybrid nanofluid over vertical stretching sheet with magnetic field effect." *CFD Letters* 14, no. 3 (2022): 39-52. https://doi.org/10.37934/cfdl.14.3.3952

[15] Qing, Jia, Bhatti Muhammad Mubashir, Abbas Munawwar Ali, Rashidi Mohammad Mehdi, and Ali Mohamed El-Sayed. "Entropy generation on MHD Casson nanofluid flow over a porous stretching/shrinking surface." *Entropy* 18, no. 4 (2016): 123 https://doi.org/10.3390/e18040123.

[16] Adhikari, RajatDas Sanatan. "Biological transmission in a magnetized reactive Casson–Maxwell nanofluid over a tilted stretchy cylinder in an entropy framework." *Chinese Journal of Physics* 86 (2023): 194-226 https://doi.org/10.1016/j.cjph.2023.10.008.

[17] Alqahtani, Aisha M, Rafique Khadija, Mahmood Zafar, Al-Sinan Bushra R, Khan Umar, and Hassan Ahmed M. "MHD rotating flow over a stretching surface: The role of viscosity and aggregation of nanoparticles." *Heliyon* 9, no. 11 (2023): https://doi.org/10.1016/j.heliyon.2023.e21107

[18] Vajravelu, KRollins D. "Heat transfer in a viscoelastic fluid over a stretching sheet." *Journal of Mathematical analysis and applications* 158, no. 1 (1991): 241-255. https://doi.org/10.1016/0022-247X(91)90280-D

[19] Maranna, T, Sachhin SM, Mahabaleshwar US, and Hatami M. "Impact of Navier's slip and MHD on laminar boundary layer flow with heat transfer for non-Newtonian nanofluid over a porous media." *Scientific Reports* 13, no. 1 (2023): 12634 https://doi.org/10.1038/s41598-023-39153-y.

[20] Puneeth, V, Ali Farhan, Khan M Riaz, Anwar M Shoaib, and Ahammad N Ameer. "Theoretical analysis of the thermal characteristics of Ree–Eyring nanofluid flowing past a stretching sheet due to bioconvection." *Biomass Conversion and Biorefinery* 14, no. 7 (2024): 8649-8660 https://doi.org/10.1007/s13399-022-02985-1

[21] Gupta, PSGupta AS. "Heat and mass transfer on a stretching sheet with suction or blowing." *The Canadian journal of chemical engineering* 55, no. 6 (1977): 744-746. https://doi.org/10.1002/cjce.5450550619

[22] Magyari, EKeller B. "Heat and mass transfer in the boundary layers on an exponentially stretching continuous surface." *Journal of Physics D: Applied Physics* 32, no. 5 (1999): 577.

[23] Elbashbeshy, EMA. "Heat transfer over an exponentially stretching continuous surface with suction." *Archives of Mechanics* 53, no. 6 (2001): 643-651.

[24] Partha, MK, Murthy PVSN, and Rajasekhar GP. "Effect of viscous dissipation on the mixed convection heat transfer from an exponentially stretching surface." *Heat and Mass transfer* 41 (2005): 360-366. https://doi.org/10.1007/s00231-004-0552-2

[25] Khan, Sujit Kumar. "Boundary layer viscoelastic fluid flow over an exponentially stretching sheet." *Applied Mechanics and Engineering* 11, no. 2 (2006): 321.

[26] Sanjayanand, EmmanuelKhan Sujit Kumar. "On heat and mass transfer in a viscoelastic boundary layer flow over an exponentially stretching sheet." *International Journal of Thermal Sciences* 45, no. 8 (2006): 819-828. https://doi.org/10.1016/j.ijthermalsci.2005.11.002

[27] Sajid, MHayat T. "Influence of thermal radiation on the boundary layer flow due to an exponentially stretching sheet." *International Communications in Heat and Mass Transfer* 35, no. 3 (2008): 347-356. https://doi.org/10.1016/j.icheatmasstransfer.2007.08.006

[28] Bidin, BilianaNazar Roslinda. "Numerical solution of the boundary layer flow over an exponentially stretching sheet with thermal radiation." *European journal of scientific research* 33, no. 4 (2009): 710-717.

[29] Bararnia, H, Gorji M, Domairry G, and Ghotbi Abdoul R. "An analytical study of boundary layer flows on a continuous stretching surface." *Acta applicandae mathematicae* 106 (2009): 125-133. https://doi.org/10.1007/s10440-008-9286-3

[30] Okonkwo, Eric C, Wole-Osho Ifeoluwa, Almanassra Ismail W, Abdullatif Yasser M, and Al-Ansari Tareq. "An updated review of nanofluids in various heat transfer devices." *Journal of Thermal Analysis and Calorimetry* 145 (2021): 2817-2872. https://doi.org/10.1007/s10973-020-09760-2

[31] Sivashanmugam, P. "Application of nanofluids in heat transfer." *An overview of heat transfer phenomena* 16 (2012): https://doi.org/10.5772/52496

[32] Xuan, YiminLi Qiang. "Heat transfer enhancement of nanofluids." *International Journal of heat and fluid flow* 21, no. 1 (2000): 58-64. https://doi.org/10.1016/S0142-727X(99)00067-3

[33] Choi, S USEastman Jeffrey A, *Enhancing thermal conductivity of fluids with nanoparticles*. 1995, Argonne National Lab.(ANL), Argonne, IL (United States). https://www.osti.gov/servlets/purl/196525.

[34] Lee, S, Choi SU-S, Li S, and, and Eastman JA. "Measuring thermal conductivity of fluids containing oxide nanoparticles." (1999): https://doi.org/10.1115/1.2825978

[35] Li, Shuguang, Faizan M, Ali Farhan, Ramasekhar Gunisetty, Muhammad Taseer, Khalifa Hamiden Abd El-Wahed, and Ahmad Zubair. "Modelling and analysis of heat transfer in MHD stagnation point flow of Maxwell nanofluid over a porous rotating disk." *Alexandria Engineering Journal* 91 (2024): 237-248. https://doi.org/10.1016/j.aej.2024.02.002

[36] Rasheed, Tahir, Hussain Tariq, Anwar Muhammad Tuoqeer, Ali Jazib, Rizwan Komal, Bilal Muhammad, Alshammari Fwzah H, Alwadai Norah, and Almuslem Amani Saleh. "Hybrid nanofluids as renewable and sustainable colloidal suspensions for potential photovoltaic/thermal and solar energy applications." *Frontiers in Chemistry* 9 (2021): 737033. https://doi.org/10.3389/fchem.2021.737033

[37] Bhattad, Atul, Atgur Vinay, Rao Boggarapu Nageswar, Banapurmath NR, Yunus Khan TM, Vadlamudi Chandramouli, Krishnappa Sanjay, Sajjan AM, Shankara R Prasanna, and Ayachit NH. "Review on mono and hybrid nanofluids: preparation, properties, investigation, and applications in IC engines and heat transfer." *Energies* 16, no. 7 (2023): 3189. https://doi.org/10.3390/en16073189

[38] Devi, SP AnjaliDevi S Suriya Uma. "Numerical investigation of hydromagnetic hybrid Cu–Al2O3/water nanofluid flow over a permeable stretching sheet with suction." *International Journal of Nonlinear Sciences and Numerical Simulation* 17, no. 5 (2016): 249-257. https://doi.org/10.1515/ijnsns-2016-0037

[39] Waini, Iskandar, Ishak Anuar, and Pop Ioan. "Hybrid nanofluid flow towards a stagnation point on a stretching/shrinking cylinder." *Scientific Reports* 10, no. 1 (2020): 9296. https://doi.org/10.1038/s41598-020-66126-2

[40] Waqas, Hassan, Naqvi Syed Muhammad Raza Shah, Alqarni MS, and Muhammad Taseer. "Thermal transport in magnetized flow of hybrid nanofluids over a vertical stretching cylinder." *Case Studies in Thermal Engineering* 27 (2021): 101219. https://doi.org/10.1016/j.csite.2021.101219

[41] Roy, Nepal Chandra, Saha Litan Kumar, and Sheikholeslami Mohsen. "Heat transfer of a hybrid nanofluid past a circular cylinder in the presence of thermal radiation and viscous dissipation." *AIP Advances* 10, no. 9 (2020): https://doi.org/10.1063/5.0021258

[42] Ali, F, Zaib A, Faizan M, Zafar SS, Alkarni Shalan, Shah Nehad Ali, and Chung Jae Dong. "Heat and mass exchanger analysis for Ree-Eyring hybrid nanofluid through a stretching sheet utilizing the homotopy perturbation method." *Case Studies in Thermal Engineering* 54 (2024): 104014. https://doi.org/10.1016/j.csite.2024.104014

[43] Ali, Farhan, Zaib A, Reddy Srinivas, Alshehri Mansoor H, and Shah Nehad Ali. "Impact of thermal radiative Carreau ternary hybrid nanofluid dynamics in solar aircraft with entropy generation: significance of energy in solar aircraft." *Journal of Thermal Analysis and Calorimetry* 149, no. 4 (2024): 1495-1513. https://doi.org/10.1007/s10973-023-12734-9

[44] Ahmed, Muhammad Faizan, Ali Farhan, Zafar Syed Sohaib, Reddy C Srivinas, and Aslam Muhammad. "Irreversibility analysis and thermal radiative of Williamson (ZnO+ MOS 2/C 3 H 8 O 2) hybrid nanofluid over a porous surface with a suction effect." *Physica Scripta* 98, no. 11 (2023): 115237.

[45] Das, Sanatan, Ali Akram, and Jana Rabindra Nath. "Numerically framing the impact of magnetic field on nanofluid flow over a curved stretching surface with convective heating." *World Journal of Engineering* 18, no. 6 (2021): 938-947. https://doi.org/10.1108/WJE-11-2020-0587

[46] Sarkar, SoumitraDas Sanatan. "Gyrotactic microorganisms swimming in magneto-Sutterby-nanofluid over a sliding cylinder set in a Darcy-Forchheimer porous space with Arrhenius kinetics." *International Journal of Ambient Energy* 45, no. 1 (2024): 2258896. https://doi.org/10.1080/01430750.2023.2258896

[47] Alkasasbeh, Hamzeh, Al Faqih Feras M, and Shoul Abedalrahman S. "Computational simulation of magneto convection flow of williamson hybrid nanofluid with thermal radiation effect." *CFD Letters* 15, no. 4 (2023): 92-105. https://doi.org/10.37934/cfdl.15.4.92105

[48] Ahmad, Syakila, Rohni Azizah Mohd, and Pop Ioan. "Blasius and Sakiadis problems in nanofluids." *Acta Mechanica* 218 (2011): 195-204. https://doi.org/10.1007/s00707-010-0414-6